Translational Oncology

www.transonc.com

Volume 4 Number 5 October 2011 pp. 301–313 301

Expression Profiling of Vulvar Carcinoma: Clues for Deranged Extracellular Matrix Remodeling and Effects on Multiple Signaling Pathways Combined with Discrete Patient Subsets[1,2]

Kalliopi I. Pappa*,†,‡, Jasmine Jacob-Hirsch§, George D. Vlachos*, Ioanna Christodoulou*, George Partsinevelos*, Ninette Amariglio§, Sofia Markaki¶, Aris Antsaklis* and Nicholas P. Anagnou†,‡

*First Department of Obstetrics and Gynecology, University of Athens School of Medicine, Alexandra Hospital, Athens, Greece; †Laboratory of Biology, Department of Basic Medical Sciences, University of Athens School of Medicine, Athens, Greece; ‡Laboratory of Cell and Gene Therapy, Center of Basic Research II, Biomedical Research Foundation of the Academy of Athens, Athens, Greece; §Cancer Research Center, The Chaim Sheba Medical Center, Tel Hashomer and Sackler School of Medicine, Tel Aviv University, Tel Aviv, Israel; ¶Department of Pathology, Alexandra Hospital, Athens, Greece

Abstract

The molecular mechanisms of vulvar squamous cell carcinoma (VSCC) remain obscure. To this end, we investigated systematically for the first time the expression profile of VSCC using the microarray technology, in a total of 11 snap-frozen samples, from five VSCC patients covering early and advanced stages of VSCC undergoing radical surgery and from six matched healthy controls. All experiments were performed using Affymetrix Human Genome U133A 2.0 oligonucleotide arrays, covering 22,277 probe sets. Genes were filtered and analyzed using analysis of variance, *t* test, fold-change calculations, and unsupervised hierarchical cluster analysis. Further processing included functional analysis and overrepresentation calculations based on Gene Ontology, Database for Annotation, Visualization, and Integrated Discovery, and Ingenuity Pathway Analysis. The molecular phenotypes of VSCC patients exhibited significant and discrete transcriptional differences from the healthy controls, whereas principal component analysis documented that this separation is mediated by a consistent set of gene expression differences. We detected 1077 genes (306 upregulated and 771 downregulated) that were differentially expressed between VSCC patients and healthy controls by at least twofold ($P < .01$), whereas a novel subset of patients was revealed displaying a distinct pattern of 125 upregulated genes involved in multiple cellular processes. Functional analysis of the 1077 genes documented their involvement in more than 50 signaling pathways, such as PTEN, oncostatin M, and extracellular signal–regulated kinase signaling, affecting extracellular matrix remodeling and invasion. Comparison of our data set with those of the single VIN study revealed that the two entities share a limited number of genes and display unique features.

Translational Oncology (2011) 4, 301–313

Address all correspondence to: Dr. Kalliopi I. Pappa, First Department of Obstetrics and Gynecology, University of Athens School of Medicine, Alexandra Hospital, 11528 Athens, Greece. E-mail: kpappa@med.uoa.gr

[1]This study was funded by the European Union Social Fund and National Resources EPEAEK II-Pythagoras II Programme (grant no. 70-3-7981 to N.P.A. and K.I.P.). The authors declare that they have no commercial affiliations or financial interests or other interests that might be perceived to influence the results and discussion reported in the article.

[2]This article refers to supplementary materials, which are designated by Tables W1 to W5 and Figures W1 and W2 and are available online at www.transonc.com.

Received 20 April 2011; Revised 20 April 2011; Accepted 6 May 2011

 1944-7124/11

DOI 10.1593/tlo.11148

Introduction

Vulvar carcinoma, although a rare form of all female genital malignancies, represents the fourth most common gynecologic cancer, exhibiting an overall incidence of approximately 1.5 per 100,000 women-years. However, this low rate increases significantly with age, reaching up to 20 per 100,000 women-years after the age of 75 [1]; histologically, the most common type is manifested as vulvar squamous cell carcinoma (VSCC), accounting for 80% to 90% of the cases [2]. In contrast to the increasing frequency of its precursor premalignant lesion, that is, vulvar intraepithelial neoplasia (VIN) [3], which is prevalent in women of relatively younger age and usually associated with human papillomavirus (HPV) infection, vulvar carcinoma remained stable during the last 40 years [1], exhibiting a rather lower overall frequency of HPV infection [4] as reflected by the individual frequencies of its four histologic subtypes [4–7]. The unique features of these two disorders have made them very informative models to investigate the actual molecular pathways resulting in the sequential transformation of the vulvar epithelium and its evolution to squamous cell carcinoma. These discrete differences also imply that, besides the HPV component required for the initial generation of VIN, additional risk factors are needed for the evolution to VSCC, including chronic vulvar inflammation, smoking, immunodeficiency status, and increasing age [8].

The recent reclassification of VIN terminology by the International Society for the Study of Vulvovaginal Diseases [9] replaced the previous three subclassifications of VIN 1 to 3 and introduced the subdivision of VIN into the (*a*) usual type, comprising the high-grade lesions 2 and 3 occurring mainly in younger women, and the (*b*) differentiated type, encompassing the previous type of differentiated VIN 3. It is of interest that this reclassification has greatly facilitated the matching of the two putative discrete pathogenetic pathways leading to the development of VSCC; the usual type requiring the presence of HPV infection, mediated by oncogenic subtypes such as 16, 18, 31, and 33, whereas the differentiated type, mostly developing in older women on a background of lichen sclerosis or squamous cell hyperplasia, does not [10]. Thus, the two resulting pathogenetic types of VSCC, which can be considered to arise from the two corresponding pathways, are the basaloid or warty type, derived from the usual VIN pathway through a long transition period, occurring in younger women and associated with HPV [11], and the keratinizing type, originating through the differentiated VIN pathway [6] through a rapid progression, occurring in older women not linked with HPV infection [3].

To clarify the precise molecular events leading to the two types of VSCC, recent studies have attempted to correlate several cell cycle–related parameters with the two pathways leading to VSCC [10,12]. In the classic form, high levels of coexpression of $p14^{ARF}$ and $p16^{INK4A}$ were found in most classic VIN lesions and were correlated with the degree of dysplasia and the presence of HPV [10], whereas most of the cases of either differentiated VIN or keratinizing VSCC were found to be negative for HPV, exhibited very low frequency of combined expression of $p14^{ARF}$ and $p16^{INK4A}$, and occurred in older women [10]. A further study by the same group [12] confirmed the previous findings and extended the capacity of accurately distinguishing the two pathways by the implementation of a robust immunohistochemical panel involving $p16^{INK4A}$, p53, and MIB1, a monoclonal antibody for the proliferation marker Ki-67. Other studies documented the role of the endothelin axis in tissue microarrays with VSCC; particularly, receptor ET_BR was found to be a prognostic factor, whereas its expression correlated with disease progression [13]. Expression of the 14-3-3-σ protein, also named stratiffin, which promotes G_2/M cell cycle arrest, was found immunohistochemically to be downregulated in a subset of VSCC, suggesting a putative role in its development [14]. Furthermore, a series of additional individual molecular markers have been investigated in VSCC, and their roles in the pathogenesis, progression, or prognosis have been extensively reviewed recently [15]. However, owing to the single-parameter approach by these limited studies, no concrete conclusions can be generated regarding the role of these markers in the pathogenesis of VSCC. Recently, a multiparameter approach using the microarray technology was used for the analysis of HPV-related VIN and documented that VIN is inherently a highly proliferative disorder, without displaying, however, dysregulation of apoptosis or angiogenesis [16].

In view of these limited data on the pathogenesis of VSCC, in the present study, we opted a systematic approach to delineate for the first time the molecular markers and the cellular pathways involved in the pathogenesis of VSCC by analyzing the gene expression profile of VSCC using the microarray technology [17].

Materials and Methods

Patients and Samples

A total of 11 snap-frozen samples were analyzed, derived from five VSCC patients undergoing radical vulvectomy with lymphadenectomy and from six matched healthy control samples of histologically normal vulvar tissue obtained by vulvar biopsy from patients undergoing surgery for benign gynecologic diseases, such as uterine prolapse. The tumor samples were classified according to the 2009 vulvar cancer staging system of the International Federation of Gynecology and Obstetrics [18] and the histologic classification system of the World Health Organization. All tissues were obtained using informed consent after the approval from the institutional ethical committee of the Alexandra Hospital. None of the patients had received any preoperative chemotherapy or irradiation treatment.

HPV DNA Genotyping

The linear-array HPV genotyping test (CE-IVD), a strip-based qualitative *in vitro* assay (Hoffmann-La Roche Ltd, Basel, Switzerland), was used for the detection of the low-risk and high-risk genotypes of HPV in vulvar cells [19]. The test uses amplification of target DNA by polymerase chain reaction and nucleic acid hybridization for the detection of 37 low-risk and high-risk genotypes of HPV. The detection of amplified DNA was performed using an array of oligonucleotide probes that permits independent identification of HPV genotypes. The method detects with high sensitivity 24 low-risk types (6, 11, 26, 40, 42, 53, 54, 55, 61, 62, 64, 66, 67, 69, 70, 71, 72, 73, 81, 82, 83, 84, IS39, and CP6180) and 13 high-risk types (16, 18, 31, 33, 35, 39, 45, 51, 52, 56, 58, 59, and 68). The method uses two internal controls of β_2-microglobulin with low and high concentration. All samples were tested twice.

RNA Preparation

Total cellular RNA from the 11 snap-frozen samples was prepared using TRIzol (Invitrogen by Life Technologies, Carlsbad, CA) and was further purified by using phenol/chloroform/isoamyl alcohol (25:24:1 vol/vol/vol) extraction [20].

Gene Expression Profiling

Experiments were performed using Affymetrix Human Genome U133A 2.0 oligonucleotide arrays (Affymetrix, Santa Clara, CA) as described (http://www.affymetrix.com/support/technical/datasheets/human_datasheet.pdf). Total RNA from each sample was used to prepare biotinylated target complementary RNA, with minor modifications from the manufacturer's recommendations (expression_manual.affx). The quality and amount of starting RNA were confirmed using an agarose gel.

Briefly, 5 μg of messenger RNA was used to generate first-strand complementary DNA by using a T7-linked oligo(dT) primer. After second-strand synthesis, *in vitro* transcription was performed with biotinylated UTP and CTP (Affymetrix), resulting in an approximately 300-fold amplification of RNA. The target complementary DNA generated from each sample was processed as per the manufacturer's recommendation using an Affymetrix GeneChip Instrument System (expression_manual.affx). Briefly, spike controls were added to 15 μg of fragmented complementary RNA before overnight hybridization. Arrays were then washed and stained with streptavidin-phycoerythrin before being scanned on an Affymetrix GeneChip scanner. After scanning, array images were assessed by eye to confirm scanner alignment and the absence of significant bubbles or scratches on the chip surface. A complete description of these technical procedures is available at the following Web site: https://www.affymetrix.com/support/technical/manuals.affx.

The individual 3′/5′ ratios for glyceraldehyde-3-phosphate dehydrogenase and β-actin were confirmed to be within acceptable limits (1.2-3.03 and 0.8-1.5, respectively), whereas BioB spike controls were found to be present on all chips, with BioC, BioD, and CreX also present in increasing intensity. When scaled to a target intensity of 150 (using Affymetrix MAS 5.0 array analysis software), scaling factors for all arrays were within acceptable limits (0.59-1.45), as were background, *Q* values, and mean intensities. Details of quality control measures can be found at http://www.ncbi.nlm.nih.gov/geo/.

Data Analysis

Gene-level RMA sketch algorithm (Partek Genomics Suite 6.5; 6.10.0810; St Louis, MO) was used for normalizing and calculating the summarized probe set values. Genes were filtered and analyzed using analysis of variance, *t* test, fold-change calculations, and unsupervised hierarchical cluster analysis (Partek Genomics Suite 6.5; 6.10.0810; and TIBCO Spotfire DecisionSite for Functional Genomics, Somerville, MA). Further processing included functional analysis and overrepresentation calculations based on Gene Ontology (GO) Annotation Tool and publication data of Database for Annotation, Visualization, and Integrated Discovery (http://david.abcc.ncifcrf.gov/) [21,22] and Ingenuity Pathway Systems. Overrepresentation calculations were performed using Ease (http://david.abcc.ncifcrf.gov/). Data results are deposited in http://www.ncbi.nlm.nih.gov/geo/. Principal component analysis (PCA) of microarray results was performed with S-plus (version 6.1; Insightful Corp, Seattle, WA; www.insightful.com/support/splus61win).

Results

Clinicopathologic Data

The clinical parameters and the histopathologic features of the patients with VSCC and of the healthy controls are summarized in Table 1. The patients covered both early and advanced stages of VSCC and displayed no tumor progression after radical vulvectomy and lymphadenectomy.

Global Expression Profile Analysis of VSCC

The global gene expression profile analysis between the samples from patients with VSCC and those from the healthy controls was performed by using the Affymetrix Human Genome U133A 2.0 microarray platform, covering 22,277 probe sets and 500,000 distinct oligonucleotide features, representing 14,500 well-characterized human genes. Initially, data were subjected to unsupervised hierarchical clustering analysis to identify subgroups of samples that may exhibit discrete molecular phenotypes. The analysis included five VSCC and six healthy control samples, each sample treated as a 22,277-dimension vector (based on the total probe sets in the array), and the Euclidean distance between samples was established and used as the metric distance. As shown in Figure 1, a clear distinction between vulvar cancer patients and healthy control individuals was documented. These data are consistent with the fact that the molecular phenotypes in vulvar cancer exhibit significant and discrete transcriptional differences from the normal.

We next investigated the presence of underlying patterns in gene expression data from the microarray experiment by performing unsupervised PCA. This linear projection method reduces the dimensionality of microarray data and permits the visualization of the relatedness between genes and/or samples that it clusters. When PCA was performed using data from 1077 differentially expressed genes, it demonstrated a dramatic separation between controls and VSCC samples as shown in Figure W1. This finding actually indicates that this separation is mediated by a consistent set of gene expression differences.

Differential Expression of VSCC-Specific Genes and a Novel Subset of VSCC Patients

On the basis of these findings, we next searched for the identification of the genes responsible for the establishment of the aberrant expression profile in VSCC, leading to a distinctive phenotype from the normal state. Using the *t* test method, we detected 1077 genes that were differentially expressed between the tumor and the normal samples by at least twofold with statistical significance ($P < .01$), as shown in Table W1, which contains a complete listing of all the differentially expressed genes. A heat map displaying the differential expression of these genes is shown in Figure 2. It is noteworthy that the downregulated genes were found to be common to all five tumor samples. However, samples 1 and 2 displayed a quite distinct pattern of upregulated genes, suggesting the presence of a putative subset operating in VSCC and exhibiting significant differences at the level of the transcriptome. These differences were further investigated among the group of the 306 upregulated genes in the tumor samples (Figure 2). Their analysis revealed a distinct set of 125 genes, with a fold change greater than 2.0 ($P < .01$) as shown in Table W2. GO analysis of the set of these upregulated 125 genes in the two tumor samples revealed that most of these genes are involved in the biologic processes of cell death, cell-to-cell signaling and interaction, cellular development, cellular growth and proliferation, cellular movement, and cellular assembly and organization. Their differential expression among the vulvar cancer samples may thus represent the basis for explaining these discrete molecular phenotypes.

Table 1. Clinicopathologic Features of the Five Patients with VSCC and of the Six Women of the Matched Healthy Control Group.

	Vulvar Tumors					Controls					
	1	2	3	4	5	1	2	3	4	5	6
Origin type	Primary	Primary	Primary	Recurrence	Primary	Uterine prolapse	Uterine prolapse	Uterine prolapse	Uterine prolapse	Uterine prolapse	Uterine prolapse
Age (y)	78	78	77	82	79	72	56	55	75	69	70
Smoker	No	No	No	No	No	No	No	No	No	No	No
Pathologic diagnosis	Keratinizing squamous carcinoma	Keratinizing squamous carcinoma	Keratinizing squamous carcinoma	Keratinizing squamous carcinoma	Basaloid squamous carcinoma	Control	Control	Control	Control	Control	Control
Tumor stage (FIGO 2009)	IB	II	II	IIIB	IIIB						
Inguinal and femoral lymph node status	Negative	Negative	Negative	Positive	Positive						
Tumor maximum diameter (cm)	1.5	3.8	5	6.5	4.8						
Histologic grade	2	1	1	1	3						
Location	Unilateral middle third	Unilateral upper third	Unilateral upper third	Bilateral multifocal	Bilateral multifocal						
VIN history	Negative	Negative	Negative	Negative	Positive						
HPV	No	No	Type 16	No	No						
5-year survival	Yes	Yes	Unknown status	Yes	Yes						
Tumor progression in 5 y											
Local recurrence	No	No	Unknown status	No	No						
Distant metastasis	No	No	Unknown status	No	No						
Death of disease	No	No	Unknown status	No	No						
Tumor unrelated death	No	No	Unknown status	No	Yes						
Type of treatment	Radical vulvectomy and bilateral inguinal and femoral node dissection	Modified radical semivulvectomy with bilateral inguinal node and femoral node dissection	Radical vulvectomy with bilateral inguinal and femoral node dissection	Radical vulvectomy with bilateral inguinal and femoral node dissection plus radiation therapy to the pelvis and groin	Radical vulvectomy with bilateral inguinal and femoral node dissection plus radiation therapy to the pelvis and groin						

FIGO indicates International Federation of Gynecology and Obstetrics.

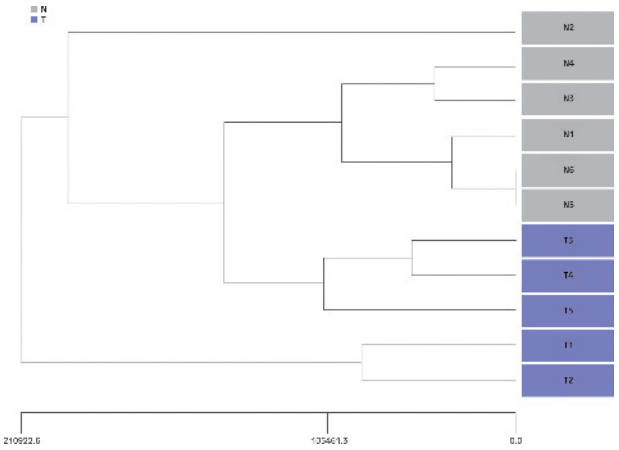

Figure 1. Agglomerative unsupervised hierarchical clustering of the microarray data from tumor and normal samples groups. Although a high diversity is seen within each group, there is a clear division between the two groups as represented by the different clusters. A distance matrix was computed using the Euclidean distance method. N indicates normal samples; T, tumor samples (VSCC).

Furthermore, of the 1077 differentially expressed genes, 306 were upregulated and 771 were downregulated compared with healthy controls, as shown in Table W1. A representative list of these genes exhibiting the highest and lowest levels of fold expression is shown in Table 2, *A* and *B*, respectively. Among these genes exhibiting marked up-regulation, there are many critical genes, such as the matrix metalloproteinases 1 and 12 (*MMP1* and *MMP12*), the interleukin 1 family member 9 (*IL1F9*), the periostin or osteoblast-specific factor (*POSTN*), the interleukin 1 alpha (*IL1A*), and interleukin 24 (*IL24*), which are well characterized as cancer markers and are involved in the process of tumorigenicity. In addition, several regulatory genes relevant to carcinogenesis displayed excessive down-regulation, such as endothelin 3 (*END3*), complement factor D (*adipsin*), the two detoxification proteins cytochrome P450, family 4, subfamily B, polypeptide 1 (*CYP4B1*) and glutathione peroxidase 3 (*GPX3*), and chemokine (C-X-C motif) ligand 12 or stromal cell–derived factor (*CXCL12*), implicated in metastasis of some cancers, and the pleiomorphic adenoma gene-like 1 (*PLAGL1*) tumor suppressor gene.

Functional Characterization of the Differentially Regulated Genes in VSCC

To functionally characterize the differentially regulated 1077 genes, we performed GO analysis using the Ingenuity Pathway Analysis software. The genes were found to be distributed among several functional classes; of the 20 identified classes, the most significant ones were cellular growth and proliferation, cell death, cellular development, cellular movement, cell cycle, and others as depicted in Table 3. A more detailed analysis of the individual number of genes exhibiting either up-regulation or down-regulation in each of the 20 functional groups is depicted in Figure 3. The most abundant upregulated genes belonged to the biologic process of cellular growth and proliferation, whereas the most downregulated genes involved the categories of cellular growth and proliferation, cell death, and cellular development.

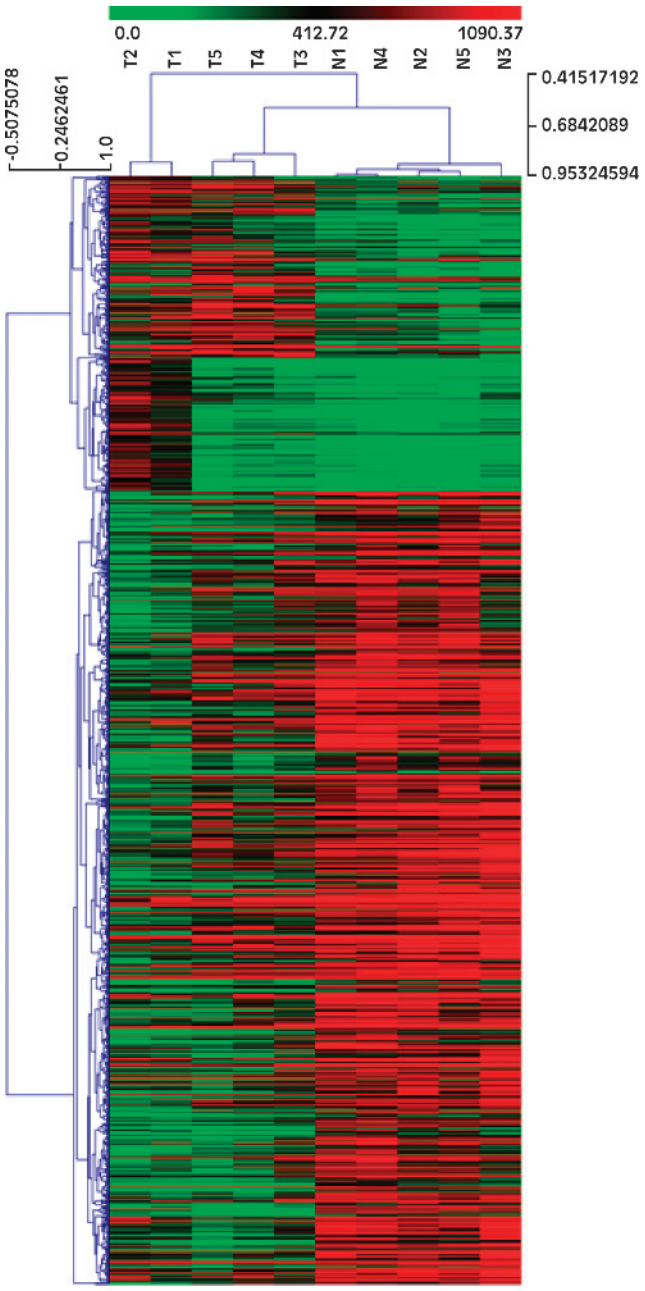

Figure 2. Hierarchical clustering of the tumor (lanes T1-T5) and normal samples (lanes N1-N5). A set of 1077 filtered genes was used to differentiate between the two groups with a threshold of at least twofold ($P < .01$). The individual lane numbers (T1-5 and N1-5) correspond to the numbers of the patients (1-5) and controls (1-5) of Table 1, respectively. There is a clear distinction between the tumor and normal samples. The downregulated probe sets are common to all tumor samples; however, tumor samples in lanes T1 and T2 display a small cluster of 125 genes with a clearly distinct pattern of up-regulation compared with tumor samples T3, T4, and T5. Unsupervised hierarchical clustering, average linkage, and Spearman rank correlation method were used for distance metric selection. Gene expression values are color coded from bright red (most up-regulated) to bright green (most downregulated).

Table 2. Top 30 Significantly Upregulated (A) and Bottom 30 Significantly Downregulated (B) Genes in VSCC.

Affymetrix ID	Gene Symbol	Description	Type(s)	Fold Change
(A) Fold change > 2, $P < .01$				
204475_at	*MMP1*	Matrix metallopeptidase 1	Peptidase	33.29
220322_at	*IL1F9*	Interleukin 1 family, member 9	Cytokine	12.13
204580_at	*MMP12*	Matrix metallopeptidase 12 (macrophage elastase)	Peptidase	11.04
210809_s_at	*POSTN*	Periostin, osteoblast specific factor	Other	10.76
210118_s_at	*IL1A*	Interleukin 1, α	Cytokine	8.69
203915_at	*CXCL9*	Chemokine (C-X-C motif) ligand 9	Cytokine	8.56
209800_at	*KRT16*	Keratin 16	Other	6.69
206569_at	*IL24*	Interleukin 24	Cytokine	6.25
202236_s_at	*SLC16A1*	Solute carrier family 16, member 1	Transporter	6.07
205943_at	*TDO2*	Tryptophan 2,3-dioxygenase	Enzyme	5.73
212365_at	*MYO1B*	Myosin IB	Other	5.05
215177_s_at	*ITGA6*	Integrin, α6	Other	4.92
214446_at	*ELL2*	Elongation factor, RNA polymerase II, 2	Transcription regulator	4.70
201490_s_at	*PPIF*	Peptidylprolyl isomerase F	Enzyme	4.55
203234_at	*UPP1*	Uridine phosphorylase 1	Enzyme	4.41
205067_at	*IL1B*	Interleukin 1, β	Cytokine	4.40
203921_at	*CHST2*	Carbohydrate sulfotransferase 2	Enzyme	4.36
202693_s_at	*STK17A*	Serine/threonine kinase 17a	Kinase	4.34
203936_s_at	*MMP9*	Matrix metallopeptidase 9	Peptidase	4.16
216918_s_at	*DST*	Dystonin	Other	4.15
211981_at	*COL4A1*	Collagen, type IV, α1	Other	4.00
211643_x_at	*IGKC*	Immunoglobulin κ constant	Other	3.91
209398_at	*HIST1H1C*	Histone cluster 1, H1c	Other	3.91
204420_at	*FOSL1*	FOS-like antigen 1	Transcription regulator	3.87
204858_s_at	*TYMP*	Thymidine phosphorylase	Growth factor	3.81
210904_s_at	*IL13RA1*	Interleukin 13 receptor, α1	Transmembrane receptor	3.68
214074_s_at	*CTTN*	Cortactin	Other	3.68
202267_at	*LAMC2*	Laminin, γ2	Other	3.64
203256_at	*CDH3*	Cadherin 3, type 1, P-cadherin (placental)	Other	3.63
206513_at	*AIM2*	Absent in melanoma 2	Other	3.62
(B) Fold change < −2, $P < .01$				
205694_at	*TYRP1*	Tyrosinase-related protein 1	Enzyme	−22.84
205382_s_at	*CFD*	Complement factor D (adipsin)	Peptidase	−15.61
208399_s_at	*EDN3*	Endothelin 3	Other	−15.58
210096_at	*CYP4B1*	Cytochrome P450, family 4, subfamily B, polypeptide 1	Enzyme	−15.22
204719_at	*ABCA8*	ATP-binding cassette, subfamily A (ABC1), member 8	Transporter	−13.79
209613_s_at	*ADH1B*	Alcohol dehydrogenase 1B (class I), β polypeptide	Enzyme	−10.84
219295_s_at	*PCOLCE2*	Procollagen C-endopeptidase enhancer 2	Other	−10.54
209318_x_at	*PLAGL1*	Pleiomorphic adenoma gene-like 1	Transcription regulator	−9.88
209687_at	*CXCL12*	Chemokine (C-X-C motif) ligand 12	Cytokine	−9.45
201348_at	*GPX3*	Glutathione peroxidase 3 (plasma)	Enzyme	−9.33
206104_at	*ISL1*	ISL LIM homeobox 1	Transcription regulator	−8.86
204731_at	*TGFBR3*	Transforming growth factor, β receptor III	Kinase	−8.56
204235_s_at	*GULP1*	GULP, engulfment adaptor PTB domain containing 1	Other	−8.53
205200_at	*CLEC3B*	C-type lectin domain family 3, member B	Other	−8.36
213397_x_at	*RNASE4*	Ribonuclease, RNase A family, 4	Enzyme	−8.30
201540_at	*FHL1*	Four-and-a-half LIM domains 1	Other	−8.25
216333_x_at	*TNXB*	Tenascin XB	Other	−8.07
207206_s_at	*ALOX12*	Arachidonate 12-lipoxygenase	Enzyme	−7.70
209894_at	*LEPR*	Leptin receptor	Transmembrane receptor	−7.69
216733_s_at	*GATM*	Glycine amidinotransferase	Enzyme	−7.68
207761_s_at	*METTL7A*	Methyltransferase like 7A	Other	−7.64
220013_at	*EPHX3*	Epoxide hydrolase 3	Enzyme	−7.64
221748_s_at	*TNS1*	Tensin 1	Other	−7.27
208335_s_at	*DARC*	Duffy blood group, chemokine receptor	G protein–coupled receptor	−7.22
201525_at	*APOD*	Apolipoprotein D	Transporter	−7.19
203706_s_at	*FZD7*	Frizzled homolog 7 (*Drosophila*)	G protein–coupled receptor	−7.18
202995_s_at	*FBLN1*	Fibulin 1	Other	−7.10
212865_s_at	*COL14A1*	Collagen, type XIV, α1	Other	−6.97
205392_s_at	*CCL14*	Chemokine (C-C motif) ligand 14	Cytokine	−6.74
209604_s_at	*GATA3*	GATA binding protein 3	Transcription regulator	−6.69

Analysis of Pathways Aberrantly Operating in VSCC

To further characterize the functional significance of the 1077 genes with the altered expression patterns, we performed a systematic analysis of the set of genes included in the list in Table W1, exhibiting a differential expression level between the two groups by at least twofold ($P < .01$), and searched for gene classifiers and pathways that are significantly enriched between the two groups by using the Ingenuity Pathway Analysis software. More than 50 signaling pathways, each involving more than five genes, were detected and considered significant ($P < .05$), documenting that VSCC affects many cytokines and signaling molecules involved in numerous signaling procedures or pathways. In the top 20 affected signaling pathways, we

Table 3. Distribution into 20 Functional Classes of the 1077 Genes Differentially Expressed between the Tumor and the Normal Samples by Twofold.

Molecular Function (GO)	No. Genes	*P*
Cellular growth and proliferation	330	7.89*e* – 07
Cell death	302	6.95*e* – 05
Cellular development	279	4.80*e* – 10
Cellular movement	225	1.07*e* – 10
Cellular assembly and organization	154	1.87*e* – 05
Cell morphology	149	3.56*e* – 07
Cell cycle	147	1.01*e* – 06
Gene expression	132	5.62*e* – 05
Small-molecule biochemistry	77	8.81*e* – 05
Posttranslational modification	66	1.18*e* – 03
Cell-to-cell signaling and interaction	57	1.18*e* – 03
Amino acid metabolism	52	6.86*e* – 04
Cellular function and maintenance	34	2.33*e* – 03
Cell signaling	29	1.93*e* – 03
Carbohydrate metabolism	28	8.81*e* – 05
Protein synthesis	28	4.69*e* – 03
Molecular transport	24	8.81*e* – 05
Lipid metabolism	7	7.83*e* – 04
Cellular compromise	7	4.76*e* – 03
Drug metabolism	3	2.56*e* – 03

located PTEN signaling (20 genes), oncostatin M signaling (10 genes), extracellular signal–regulated kinase (ERK) signaling (14 genes), and other significant pathways related to cancer as shown in Figure W2. Specifically, the pathway analysis tool revealed that the most significantly upregulated pathway in VSCC was the one related to interleukin 6 (IL-6) signaling and oncostatin M signaling, with the involvement of key regulatory genes, such as *MMP1* and *MMP12*, and *NRAS*, affecting major cellular processes, such as cell adhesion, extracellular matrix (ECM) remodeling, and invasion, as shown in Figure 4.

In addition, significant differences were found also among genes playing a key role in the regulation of cell division. Both cell division cycle 25 homologs C and B (*CDC25C* and *CDC25B*) were found to be markedly upregulated by 1.64- and 2.01-fold, respectively, among the VSCC samples compared with healthy controls ($P < .05$), as shown in Figure 5. These two genes have been recently documented to play a crucial role in the pathogenesis and progression of VSCC [23]. The network generated by the key upregulated and downregulated genes affected by *CDC25C* and *CDC25B* is depicted in Figure 6. One of the major interactors of CDC25, the androgen receptor (*AR*), was found to be significantly downregulated in the VSCC samples by 3.59-fold. This finding, combined with the most excessive down-regulation of an important member of a cell proliferation axis

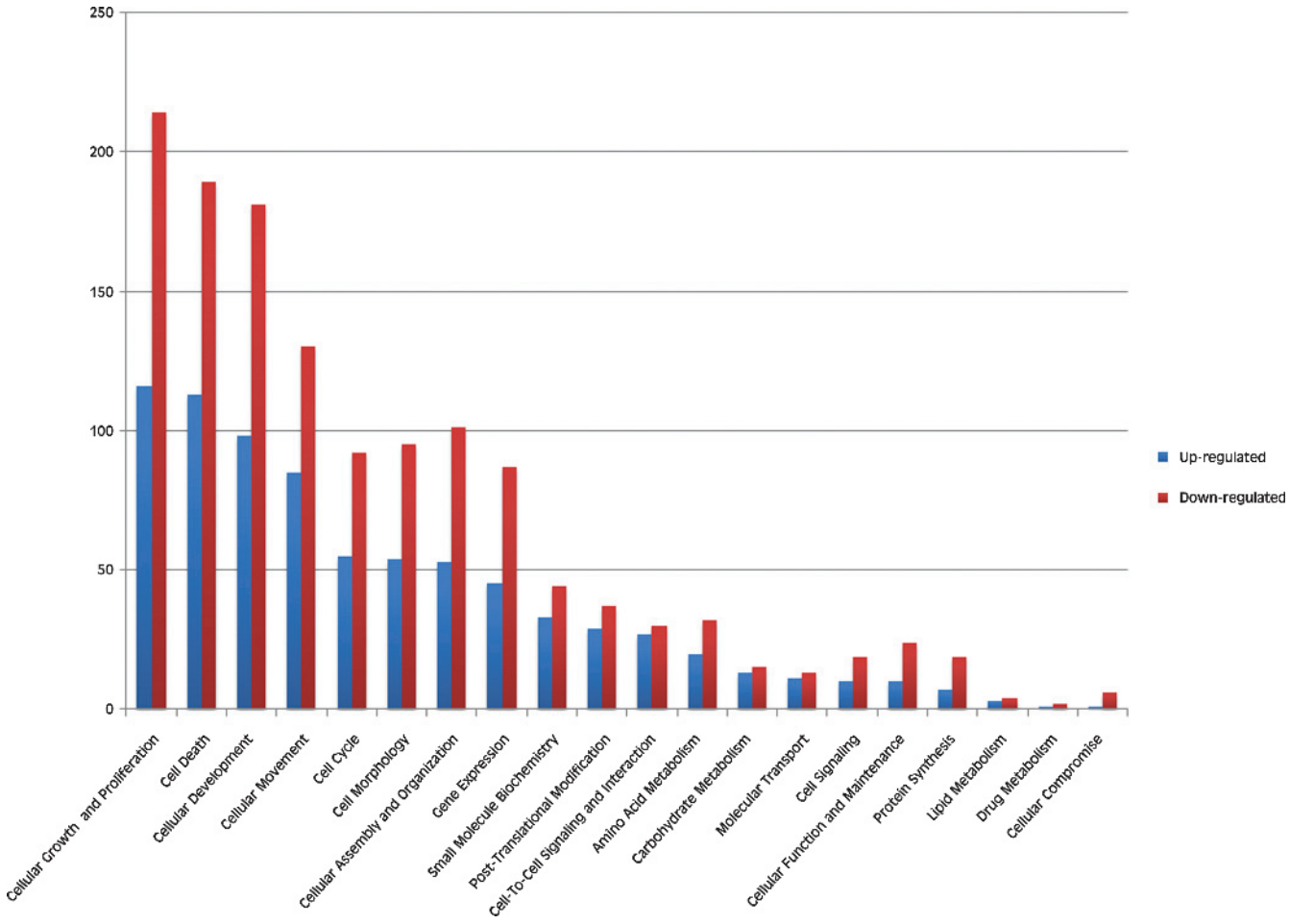

Figure 3. Functional grouping of the 1077 filtered genes differentiating between the two groups. The filtered genes exhibited either up-regulation (blue bars) or down-regulation (red bars) with a threshold of at least twofold ($P < .01$). The numbers on the *y* axis denote the total number of genes in each functional class that are either upregulated (blue) or downregulated (red).

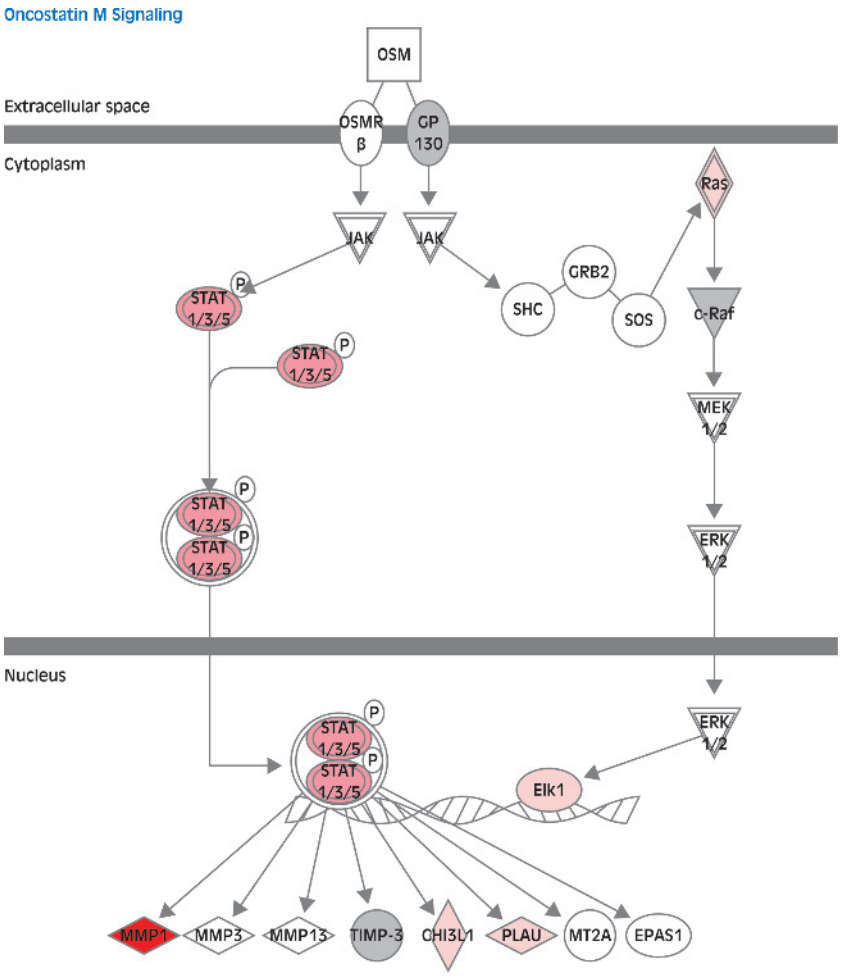

Figure 4. Oncostatin M signaling pathway. Within this pathway, the network of cell adhesion and extracellular remodeling is the most significantly upregulated network in VSCC. The latter was generated from critical genes most upregulated in the tumor samples, depicting the major nodes of MMPs 1, 2, and 13 and their interactors. Red depicts the genes that are upregulated in tumor samples. The intensity of the colors indicates the magnitude of regulation.

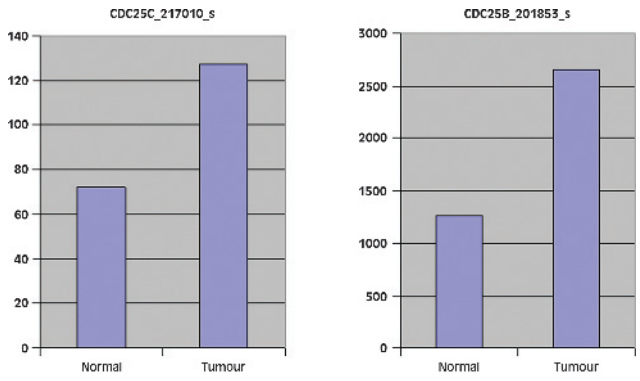

Figure 5. Up-regulation at the transcriptional level of *CDC25C* and *CDC25B* genes in the samples of VSCC compared with healthy controls. The corresponding probe sets of the Affymetrix Human Genome U133A 2.0 oligonucleotide arrays were used for this comparison. The numbers at the *y* axis indicate arbitrary units.

such as endothelin 3 (*EDN3*) by 15.58-fold and its receptor type B (*EDNRB*) by 4.34-fold, as shown in Tables 2*B* and W1, is consistent with an aberrant reduction of paracrine and endocrine functions of the tumor cells (Figure 6). A more systematic analysis to this direction, using the pathway analysis tool, revealed another important network generated by genes exhibiting significant down-regulation in the VSCC samples and involving the *AR* gene (Figure 7). Interestingly, the genes affected and interacting with the *AR* gene are related to (*a*) cancer, such as the *ZMIZ1* gene regulating the activity of various transcription factors, including Smad3/4 and p53 and associated with acute lymphoblastic leukemia, and the *ARMCX2* gene, a member of the ALEX family of proteins playing a role in tumor suppression; and (*b*) signal transduction such as the *IL6ST*, a signal transducer shared by many cytokines, including IL-6, ciliary neurotrophic factor, leukemia inhibitory factor, and oncostatin M.

Comparative Analysis of the Data Set to Proposed Markers for VSCC

On the basis of the limited available data of molecular markers for vulvar carcinoma found to be important either in the pathogenesis

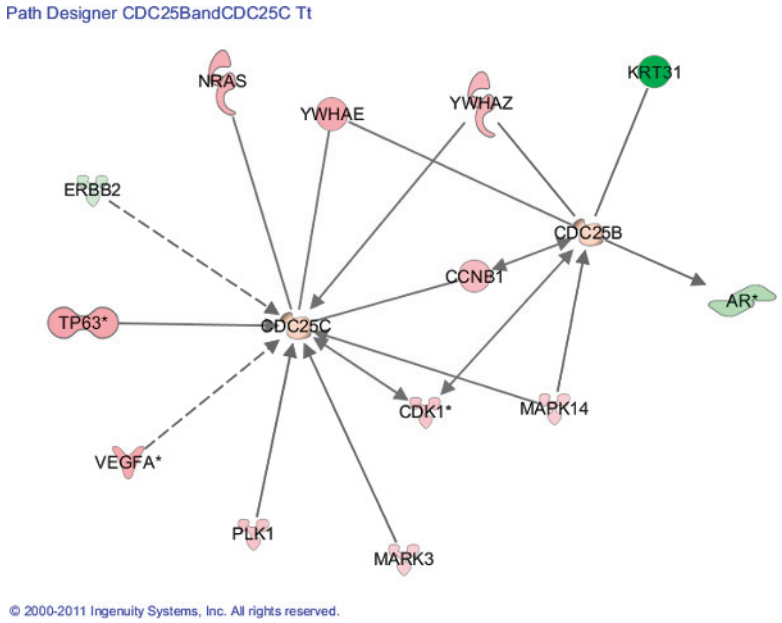

Figure 6. Network of cycle control highlighting the up-regulation of the key homologs *CDC25C* and *CDC25B* and their interacting components involved in cell cycle control, proliferation, and nuclear signaling. Note the significant down-regulation of *AR* directly affected by *CDC25B*. Solid lines indicate direct interactions; dashed lines, indirect interactions.

and/or in the progression or in the clinical outcome of vulvar carcinoma [15], we have analyzed our data for the aberrant expression of such proposed markers. Our search actually documented a limited list of such proposed genes, exhibiting significant changes in their expression profile, as shown in Table W3. Of these genes, the *VEGFA* gene, inducing angiogenesis and promoting cell migration, and the antiapoptotic *BCL2* gene displayed the most upregulated and downregulated expression, respectively.

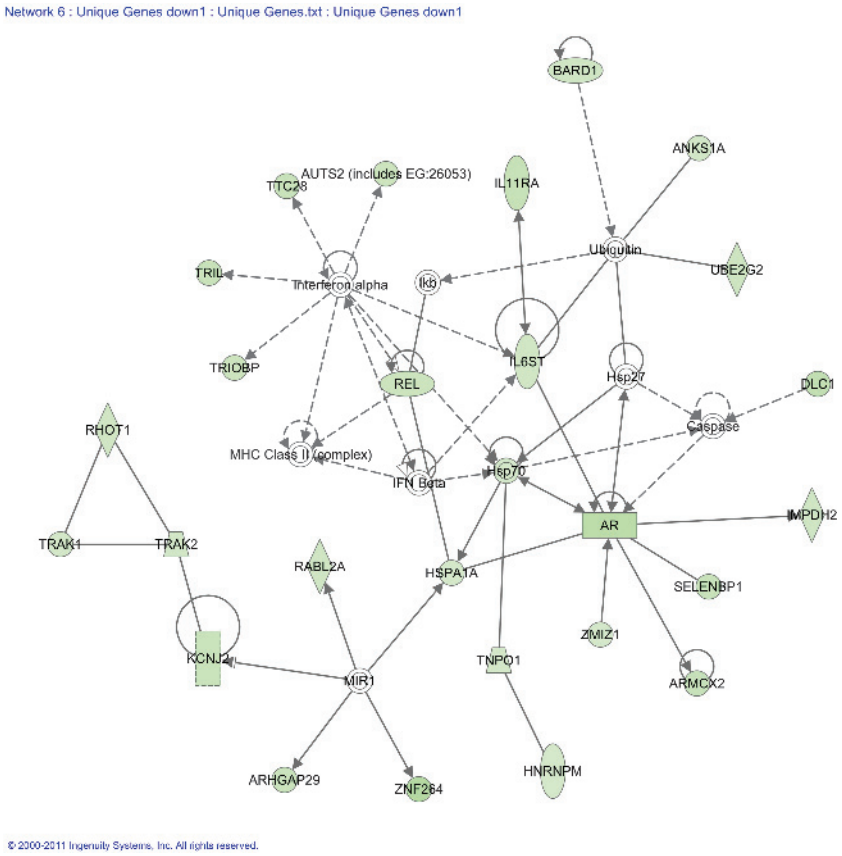

Figure 7. Network generated from the genes downregulated in the tumor samples. The genes present in the network include *AR* and its direct interactors. The network also contains genes related to cancer, inflammatory disease, and connective tissue disorders.

Figure 8. Venn diagram showing the identification of the 21 common genes upregulated both in the VIN [16] and in the present study of VSCC patients. The identified 21 genes are mostly involved in the biologic processes of cell cycle, DNA replication, recombination and repair, and cell death. Results were obtained by applying the Student's *t* test. A cutoff of .01 for the adjusted *P* value was applied. Circle radii (light blue for VIN; light orange for VSCC) are proportional to the number of transcripts differentially expressed in each condition.

Comparative Analysis of the VSCC versus *the VIN Data Set*

Because our study is the first one to systematically analyze the transcriptional profile of vulvar carcinoma, and in view of the fact that there is only one study in the literature on the precursor of vulvar carcinoma, that is, VIN [16], using the same approach, we performed a direct comparison between the two data sets. From the 1497 genes significantly changed in the VIN data set, there are 158 common genes present within the gene list generated from our samples. Of these, 21 genes were upregulated in both VIN and VSCC (Table W4 and Figure 8), whereas 121 genes were significantly downregulated in both clinical entities (Table W5 and Figure 9). Only 18 genes showed a different expression profile in the two data sets. Using the Wilcoxon signed rank test, the gene expression levels of the upregulated genes between the VIN and VSCC data sets did not differ between the two entities ($P > .10$). Most of the common upregulated genes are involved in functions related with cell cycle, DNA replication, recombination and repair, and cell death. In the 121 common downregulated genes, using the Wilcoxon signed rank test, the decrease in the level of expression was higher in VSCC ($P < .001$). Most of those genes were found to be related with cellular development (*PLAG1*), cellular movement (*FHL1*), and cellular growth and proliferation (*TGFBR3*).

Furthermore, it is noteworthy that several key gene regulators of cell proliferation, such as the glutathione peroxidase 3 (*GPX3*), which functions in the detoxification of hydrogen peroxide, the tumor suppressor *PLAG1* and the *RNASE4* gene playing an important role in messenger RNA cleavage, displayed a pattern of gradual but pronounced quantitative down-regulation from VIN to VSCC (Tables W4 and W5), implying that this evolving differential expression reflects the operating aberrant specific molecular events and mechanisms, leading eventually to the vulvar carcinoma status.

Discussion

In the present study, we performed a comprehensive analysis of the VSCC transcriptome and compared it to that of a matched normal vulvar epithelium. To our knowledge, this is the first study to describe the expression profile of this important form of cancer in a cohort of well-characterized VSCC patients of different clinical stages and histopathologic types. In view of the limited data on the pathogenesis of VSCC, our primary goal was to delineate the molecular parameters and reveal the cellular pathways involved in the pathogenesis of VSCC by using the microarray technology [17]. Our secondary aim was to compare the expression profile of the established stage of VSCC to that of its well-studied precursor, namely, the VIN, thanks to the available data of the single molecular study performed up-to-date [16], to gain insights into the evolutionary pathways of vulvar carcinogenesis. We have documented a high number of upregulated

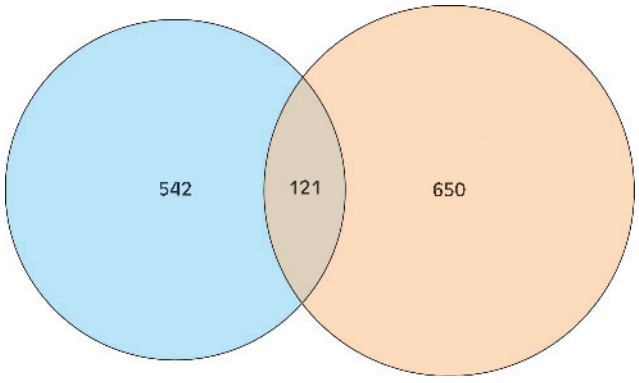

Figure 9. Venn diagram showing the identification of the 121 common genes downregulated both in the VIN [16] and in the present study of VSCC patients. The identified 121 genes are involved in the Wnt/β-catenin signaling (TCF4 transcription factor), in human embryonic stem cell pluripotency signaling pathway, like the *FGFR1* gene, and in acute myeloid leukemia signaling, like the *KIT* gene. A cutoff of .01 for the adjusted *P* value was applied. Circle radii (light blue for VIN; light orange for VSCC) are proportional to the number of transcripts differentially expressed in each condition.

and downregulated genes in VSCC affecting primarily the biologic processes of cellular growth and proliferation and specifically those of ECM remodeling and invasion and cell cycle proliferation pathways. These data are in contrast to those of the VIN expression profile [16], which are mainly characterized by increased proliferation and decreased cell communication processes.

The VSCC status induced a coordinated and aberrant expression of multiple genes involved primarily in cell growth and proliferation and in cell death, affecting more than 50 signaling pathways. The most important characteristic feature of the aberrant expression profile of the 1077 studied genes in our series of VSCC, reflecting an extensive ECM remodeling, was the pronounced up-regulation of two members of the MMP family, namely, *MMP1* and *MMP12*, and, to a lesser extent, of two additional members, namely, *MMP9* and *MMP11*, composed of more than 28 enzymes and representing the major proteases with the ability to degrade most of the components of the ECM, through a combined cleavage and release of bioactive molecules, which promote invasion and angiogenesis [24]. This activity leads to extensive ECM remodeling and cell migration. The latter function is an essential step for tumor invasion and metastasis [24], and thus, their role in the later stages of tumor development is consistent with the clinical stages of our patients (Table 1). It is noteworthy that besides these unique properties of MMPs exerted at the late stages of tumorigenesis, MMPs have been shown recently to affect also cellular signaling pathways activated at the early stages of tumor formation, by stimulating epithelial-mesenchymal transition during tumorigenesis, although the identification of the cell surface targets of MMPs in inducing epithelial-mesenchymal transition has not yet been accomplished [25]. It is important to note that there is no consistent pattern of MMP expression in the various types of cancers studied, suggesting an intrinsic tissue heterogeneity of the various parameters of ECM components [25]. In our study, within the context of the oncostatin M signaling pathway, *MMP1* and *MMP12* exhibited primarily a significant up-regulation, along with a moderate up-regulation of *MMP9* and *MMP11* (Table 2*A* and Figure 4). Particularly, *MMP1* or interstitial collagenase gene encodes a secreted enzyme cleaving interstitial collagens, types I, II and III, whereas *MMP12* or macrophage elastase encodes for an enzyme that degrades soluble and insoluble elastin and participates with other MMPs in the ECM remodeling. *MMP9* or gelatinase B, conversely, may play an essential role in local proteolysis of the ECM and in leukocyte migration and degrades fibronectin, whereas *MMP11* or stromelysin 3, codes for an enzyme, which is activated intracellularly by furin within the constitutive secretory pathway. Also, in contrast to other MMPs, this enzyme cleaves α_1-proteinase inhibitor but weakly degrades structural proteins of the ECM.

The high expression of these four MMPs in VSCC represents a genuine feature of advanced cancer status; however, this extensive remodeling seems to be mediated also by the reduced expression of the natural tissue inhibitors of metallopeptidases (TIMPs), which normally reduce excessive proteolytic ECM degradation by MMPs, thus controlling the extent of remodeling. Actually, this is corroborated in our studies by the significant down-regulation of the *TIMP3* gene by more than fivefold (Table W1 and Figure 4). Although the aberrant expression of MMPs has been associated with poor prognosis [25], in our series, all five patients have accomplished a more than 5-year survival period and had no local recurrence or distant metastases. Apparently, this can be partly attributed to the rather early clinical stages and the prompt radical treatment they all received, involving bilateral inguinal and femoral node dissection (Table 1).

Another key gene that has exhibited a significant up-regulation in VSCC, a feature compatible with the concept of invasive phenotype, was periostin or osteoblast specific factor (*POSTN*), a mesenchyme-specific gene inducing cell attachment and playing an important role in cell adhesion. The inducible overexpression of *POSTN* in tumor cell lines can lead to significant tumor progression and angiogenesis in immunocompromised animals. The latter effect seems to be mediated through an integrin $\alpha_v\beta_3$–focal adhesion kinase signaling pathway [26]. This interesting mechanism of acquired angiogenesis by *POSTN* leading to tumor promotion may thus represent a crucial role in the advanced stages of VSCC. However, it should be noted that other studies in bladder cancer have shown that *POSTN* is significantly downregulated and suppresses cell invasiveness and metastasis of cancer cells through the TAB1/TAK1 signaling pathway [27]. Thus, it is conceivable that these differences might reflect the operation of additional tissue-specific factors of the individual tumor types, interacting with the two discrete signaling pathways.

Within the context of the major pathways affected in VSCC, such as the cellular growth and proliferation and cell cycle (Figure 3), the two major homologs of cell division cycle 25, namely, *CDC25C* and *CDC25B*, were found to display moderate but significant up-regulation, affecting the control of cell cycle and other key regulators in the involved networks (Figure 6). *CDC25B* is a member of the CDC25 family of phosphatases and activates the cyclin-dependent kinase CDC2 by removing two phosphate groups and is required for entry into mitosis. *CDC25B* has oncogenic properties, although its role in tumor formation has not been determined. Multiple transcript variants for this gene exist. *CDC25C*, however, plays a much more important role in cell cycle by directing dephosphorylation of cyclin B–bound CDC2 and triggering entry into mitosis. It is also thought to suppress p53-induced growth arrest. These features make CDC25 phosphatases key participants in the process of malignant transformation after their abnormal expression. Their overexpression in several types of human cancer has been previously detected but not in vulvar cancer [28]. Recently, however, *CDC25C* and phosphorylated *CDC25C* (Ser216) were found to play a major role, whereas *CDC25B* was found to play a minor role in the pathogenesis and progression of VSCC. Overexpression of all three forms occurring at a later clinical stage was associated with an aggressive phenotype and poor prognosis [23]. Interestingly, the three isoforms were not independently correlated to prognosis, indicating that they may operate through independent pathways [28]. Actually, in our series of VSCC, the up-regulation of *CDC25C* and *CDC25B* was moderate occurring in rather early clinical stages and was associated with a rather good prognosis and survival, consistent with data of a Norwegian study [23].

The gene coding for the potent vasoactive ligand endothelin 3 (*EDN3*) has been found to display one of the most pronounced down-regulation, that is, −15.58-fold among the 1077 differentially expressed genes in our VSCC series. This was followed also by a concomitant down-regulation of endothelin 1 (*EDN1*) and their receptors *EDNRB* and *EDNRA*, by −1.36-, −4.34-, and −1.61-fold, respectively. Interestingly, a pattern of similar magnitude has been documented in the VIN study [16], where *EDN3*, *EDNRB*, and *EDNRA* exhibited a significant down-regulation of their expression by −12.1-, −2.2-, and −3.1-fold, respectively. Considering the

precancerous state of VIN, data from the VIN study and from our study document that the operation of the so-called ET axis is affected at the earliest steps of vulvar carcinogenesis, within the context of decreased communication, occurring both in VIN [16] and in cancer in general [29] and thus do not lend support to recent findings based on a semiquantitative immunohistochemical analysis on the relative expression of *EDN1* and *EDNRB* in early stages of vulvar cancer [13].

Regarding the genomic status of the vulvar neoplasia and the resulting recurrent imbalance in VSCC, of the 10 most upregulated genes in our study (Table 2*A*), the expression of *IL24* and *SLC16A1* combined with their genomic location at 1q32 and 1p12, respectively, is consistent with the recently observed gain events in the chromosomal regions 1p and 1q in VSCC using high-resolution genomic profiling [30]. Similarly, the down-regulation of *GPX3*, *CXCL12*, and *CLEC3B* located at 5q33.1, 10q11.21, and 3p21-31, respectively, is consistent with the independently observed rather infrequent (17%-33%) deletions of the corresponding chromosomal regions in a limited number of VSCC cases [30].

The evolution of VIN to VSCC through two discrete pathways represents an ideal model to identify the basic molecular mechanisms leading to the established cancerous state. Most of our patients belonged histologically to the keratinizing type, which results through a rapid progression from the differentiated VIN pathway. Both the advanced age of the patients and the lack of linkage to HPV infection are consistent with this evolutionary pathway [3]. A single patient (patient 5 in Table 1) belonged histologically to the basaloid type of VSCC, believed to derive through the classic VIN pathway. Actually, this was the only patient with an established record of VIN (Table 1). However, the pattern of differential expression of the 1077 genes that were analyzed was not different from the rest of the samples derived through the differentiated VIN pathway (Figure 2). These data imply that, at the status of VSCC, the molecular phenotypes of the end points of the two pathways exhibit similar sets of differentially expressed genes. Comparison of the whole data sets of the VIN study [16] with our study revealed only 158 common genes present in both sets. Of these, 21 genes exhibited common up-regulation and 121 common down-regulation, thus establishing for the first time the discrete pattern of gene expression between the two entities. Furthermore, several genes involved in detoxification, tumor suppression, and RNA cleavage, among others, displayed a significant gradual down-regulation during the transition from VIN to VSCC, a pattern consistent with the anticipated operating mechanisms of sequential carcinogenesis [29].

Our study revealed also for the first time the presence of a subset of VSCC patients, regardless of the clinical stage or pathologic diagnosis, exhibiting a unique set of 125 upregulated genes involved in cell death, cell-to-cell signaling and interaction, cellular development, cellular growth and proliferation, cellular movement, and cellular assembly and organization (Figure 2 and Table W2). These data provide the impetus for further studies on the functional role of this set of genes on the natural history of the disease and on the elucidation of the mechanisms for the generation of these molecular phenotypes.

In conclusion, in the present study, we have documented that vulvar neoplasia, and specifically VSCC, is consistent with a status of abnormal cell signaling, proliferation, and remodeling of ECM, being quite distinct from the described features of its premalignant state of VIN.

Acknowledgments

The authors thank Alexandros Polyzos for his invaluable help in the bioinformatics analysis and Lindy A.M. Santegoets for sharing the microarray data of VIN.

References

[1] Sturgeon SR, Brinton LA, Devesa SS, and Kurman RJ (1992). *In situ* and invasive vulvar cancer incidence trends (1973 to 1987). *Am J Obstet Gynecol* **166**, 1482–1485.

[2] Hørding U, Junge J, Daugaard S, Lundvall F, Poulsen H, and Bock JE (1994). Vulvar squamous cell carcinoma and papillomaviruses: indications for two different etiologies. *Gynecol Oncol* **52**, 241–246.

[3] McCluggage WG (2009). Recent developments in vulvovaginal pathology. *Histopathology* **54**, 56–73.

[4] Skapa P, Zamecnik J, Hamsikova E, Salakova M, Smahelova J, Jandova K, Robova H, Rob L, and Tachezy R (2007). Human papillomavirus (HPV) profiles of vulvar lesions: possible implications for the classification of vulvar squamous cell carcinoma precursors and for the efficacy of prophylactic HPV vaccination. *Am J Surg Pathol* **31**, 1834–1843.

[5] Lerma E, Matias-Guiu X, Lee SJ, and Prat J (1999). Squamous cell carcinoma of the vulva: study of ploidy, HPV, p53, and pRb. *Int J Gynecol Pathol* **18**, 191–197.

[6] Toki T, Kurman RJ, Park JS, Kessis T, Daniel RW, and Shah KV (1991). Probable nonpapillomavirus etiology of squamous cell carcinoma of the vulva in older women: a clinicopathologic study using *in situ* hybridization and polymerase chain reaction. *Int J Gynecol Pathol* **10**, 107–125.

[7] Trimble CL, Hildesheim A, Brinton LA, Shah KV, and Kurman RJ (1996). Heterogeneous etiology of squamous carcinoma of the vulva. *Obstet Gynecol* **87**, 59–64.

[8] Crum CP, McLachlin CM, Tate JE, and Mutter GL (1997). Pathobiology of vulvar squamous neoplasia. *Curr Opin Obstet Gynecol* **9**, 63–69.

[9] Sideri M, Jones RW, Wilkinson EJ, Preti M, Heller DS, Scurry J, Haefner H, and Neill S (2005). Squamous vulvar intraepithelial neoplasia: 2004 modified terminology, ISSVD Vulvar Oncology Subcommittee. *J Reprod Med* **50**, 807–810.

[10] van der Avoort IAM, Shirango H, Hoevenaars BM, Grefte JM, de Hullu JA, de Wilde PC, Bulten J, Melchers WJ, and Massuger LF (2006). Vulvar squamous cell carcinoma is a multifactorial disease following two separate and independent pathways. *Int J Gynecol Pathol* **25**, 22–29.

[11] Kurman RJ, Toki T, and Schiffman MH (1993). Basaloid and warty carcinomas of the vulva. Distinctive types of squamous cell carcinoma frequently associated with human papillomaviruses. *Am J Surg Pathol* **17**, 133–145.

[12] Hoevenaars BM, van der Avoort IA, de Wilde PC, Massuger LF, Melchers WJ, de Hullu JA, and Bulten J (2008). A panel of $p16^{INK4A}$, MIB1 and p53 proteins can distinguish between the 2 pathways leading to vulvar squamous cell carcinoma. *Int J Cancer* **123**, 2767–2773.

[13] Eltze E, Bertolin M, Korsching E, Wülfing P, Maggino T, and Lellé R (2007). Expression and prognostic relevance of endothelin-B receptor in vulvar cancer. *Oncol Rep* **18**, 305–311.

[14] Wang Z, Tropè CG, Suo Z, Trøen G, Yang G, Nesland JM, and Holm R (2008). The clinicopathological and prognostic impact of 14-3-3σ expression on vulvar squamous cell carcinomas. *BMC Cancer* **8**, 308.

[15] Knopp S, Tropè C, Nesland JM, and Holm R (2009). A review of molecular pathological markers in vulvar carcinoma: lack of application in clinical practice. *J Clin Pathol* **62**, 212–218.

[16] Santegoets LAM, Seters M, Helmerhorst TJ, Heijmans-Antonissen C, Hanifi-Moghaddam P, Ewing PC, van Ijcken WF, van der Spek PJ, van der Meijden WI, and Blok LJ (2007). HPV related VIN: highly proliferative and diminished responsiveness to extracellular signals. *Int J Cancer* **121**, 759–766.

[17] Pappa KI and Anagnou NP (2005). Emerging issues of the expression profiling technologies for the study of gynecologic cancer. *Am J Obstet Gynecol* **193**, 908–918.

[18] Mutch DG (2009). The new FIGO staging system for cancers of the vulva, cervix, endometrium, and sarcomas. *Gynecol Oncol* **115**, 325–328.

[19] Woo YL, Damay I, Stanley M, Crawford R, and Sterling J (2007). The use of HPV linear array assay for multiple HPV typing on archival frozen tissue and DNA specimens. *J Virol Methods* **142**, 226–230.

[20] Chomczynski P and Mackey K (1995). Short technical reports. Modification of the TRI reagent procedure for isolation of RNA from polysaccharide- and proteoglycan-rich sources. *Biotechniques* **19**, 942–945.

[21] Huang DW, Sherman BT, and Lempicki RA (2009). Systematic and integrative analysis of large gene lists using DAVID bioinformatics resources. *Nat Protoc* **4**, 44–57.
[22] Dennis G Jr, Sherman BT, Hosack DA, Yang J, Gao W, Lane HC, and Lempicki RA (2003). DAVID: Database for Annotation, Visualization, and Integrated Discovery. *Genome Biol* **4**, P3.
[23] Wang Z, Trope CG, Flørenes VA, Suo Z, Nesland JM, and Holm R (2010). Overexpression of CDC25B, CDC25C and phospho-CDC25C (Ser216) in vulvar squamous cell carcinomas are associated with malignant features and aggressive cancer phenotypes. *BMC Cancer* **10**, 233.
[24] Golubkov VS and Strongin AY (2007). Proteolysis-driven oncogenesis. *Cell Cycle* **6**, 147–150.
[25] Orlichenko LS and Radisky DC (2008). Matrix metalloproteinases stimulate epithelial-mesenchymal transition during tumor development. *Clin Exp Metastasis* **25**, 593–600.
[26] Shao R, Bao S, Bai X, Blanchette C, Anderson RM, Dang T, Gishizky ML, Marks JR, and Wang XF (2004). Acquired expression of periostin by human breast cancers promotes tumor angiogenesis through up-regulation of vascular endothelial growth factor receptor 2 expression. *Mol Cell Biol* **24**, 3992–4003.
[27] Isono T, Kim CJ, Ando Y, Sakurai H, Okada Y, and Inoue H (2009). Suppression of cell invasiveness by periostin via TAB1/TAK1. *Int J Oncol* **35**, 425–432.
[28] Boutros R, Lobjois V, and Ducommun B (2007). CDC25 phosphatases in cancer cells: key players? Good targets? *Nat Rev Cancer* **7**, 495–507.
[29] Hanahan D and Weinberg RA (2000). The hallmarks of cancer. *Cell* **100**, 57–70.
[30] Purdie KJ, Harwood CA, Gibbon K, Chaplin T, Young BD, Cazier JB, Singh N, Leigh IM, and Proby CM (2010). High resolution genomic profiling of human papillomavirus–associated vulval neoplasia. *Br J Cancer* **102**, 1044–1051.

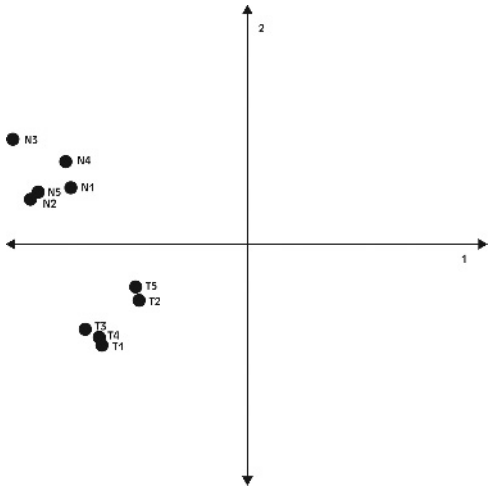

Figure W1. PCA of the 1077 significant genes. This set of genes displayed either a greater than 2-fold or a less than −2-fold change of differential expression ($P < .01$). The first two components (1 and 2) can capture 92.8% of the variability of the samples. The separation between tumor samples (T1, T2, T3, T4, T5) and normal samples (N1, N2, N3, N4, N5) can be seen from the first component.

Table W2. Distinct Set of 125 Genes Differentially Upregulated among the VSCC Patients.

Affymetrix ID	Symbol	Entrez Gene Name	Type(s)	Fold Change	*P*
204322_at	*GOLIM4*	Golgi integral membrane protein 4	Other	6.50	.00
207036_x_at	*GRIN2D*	Glutamate receptor, ionotropic, *N*-methyl D-aspartate 2D	Ion channel	5.90	.00
216419_at	*CROCC*	Ciliary rootlet coiled coil, rootletin	Other	5.54	.00
205285_s_at	*FYB*	FYN binding protein	Other	5.36	.00
210850_s_at	*ELK1*	ELK1, member of ETS oncogene family	Transcription regulator	5.04	.00
211652_s_at	*LBP*	Lipopolysaccharide binding protein	Transporter	5.00	.00
220204_s_at	*BMP8A*	Bone morphogenetic protein 8a	Growth factor	4.97	.00
210523_at	*BMPR1B*	Bone morphogenetic protein receptor, type IB	Kinase	4.89	.00
207412_x_at	*CELP*	Carboxyl ester lipase pseudogene	Other	4.68	.00
214750_at	*PLAC4*	Placenta-specific 4	Other	4.67	.00
217150_s_at	*NF2*	Neurofibromin 2 (merlin)	Other	4.66	.00
205914_s_at	*GRIN1*	Glutamate receptor, ionotropic, *N*-methyl D-aspartate 1	Ion channel	4.63	.00
204907_s_at	*BCL3*	B-cell CLL/lymphoma 3	Transcription regulator	4.53	.00
217070_at	*MTHFR*	Methylenetetrahydrofolate reductase (NAD[P]H)	Enzyme	4.51	.00
213277_at	*ZFP36L1*	Zinc finger protein 36, C3H type-like 1	Transcription regulator	4.37	.00
207312_at	*PHKG1*	Phosphorylase kinase, γ1 (muscle)	Kinase	4.35	.00
207915_at	*LOC100293553*	Similar to L-*myc*-2 protein	Other	4.35	.00
220209_at	*PYY2*	Peptide YY, 2 (seminal plasmin)	Other	4.27	.00
206602_s_at	*HOXD3*	Homeobox D_3	Transcription regulator	4.25	.00
215538_at	*LARGE*	Like-glycosyltransferase	Enzyme	4.19	.00
207462_at	*GLRA2*	Glycine receptor, α2	Ion channel	4.18	.00
221285_at	*ST8SIA2*	ST8 α-*N*-acetyl-neuraminide α-2,8-sialyltransferase 2	Enzyme	4.09	.00
215771_x_at	*RET*	Ret proto-oncogene	Kinase	4.05	.00
216838_at	*LOC92249*	Hypothetical LOC92249	Other	4.04	.00
220423_at	*PLA2G2D*	Phospholipase A2, group IID	Enzyme	4.03	.00
220657_at	*KLHL11*	Kelch-like 11 (*Drosophila*)	Other	3.91	.00
214485_at	*ODF1*	Outer dense fiber of sperm tails 1	Other	3.89	.00
221313_at	*GPR52*	G protein–coupled receptor 52	G protein–coupled receptor	3.87	.00
208571_at	*ANP32A*	Acidic (leucine-rich) nuclear phosphoprotein 32 family, member A	Other	3.84	.00
207366_at	*KCNS1*	Potassium voltage-gated channel, delayed-rectifier, subfamily S, member 1	Ion channel	3.82	.00
207138_at	*PHF2*	PHD finger protein 2	Other	3.81	.00
208157_at	*SIM2*	Single-minded homolog 2 (*Drosophila*)	Transcription regulator	3.81	.00
204179_at	*MB*	Myoglobin	Transporter	3.77	.00
204535_s_at	*REST*	RE1-silencing transcription factor	Transcription regulator	3.76	.00
215292_s_at	*MKL1*	Megakaryoblastic leukemia (translocation) 1	Transcription regulator	3.69	.00
206892_at	*AMHR2*	Anti–mullerian hormone receptor, type II	Kinase	3.68	.00
220445_s_at	*CSAG2*	CSAG family, member 2	Other	3.66	.00
205177_at	*TNNI1*	Troponin I type 1 (skeletal, slow)	Other	3.63	.00
206798_x_at	*DLEC1 (includes EG:9940)*	Deleted in lung and esophageal cancer 1	Other	3.61	.00
206768_at	*RPL3L*	Ribosomal protein L3-like	Other	3.59	.00
210326_at	*AGXT*	Alanine-glyoxylate aminotransferase	Enzyme	3.59	.00
211484_s_at	*DSCAM*	Down syndrome cell adhesion molecule	Other	3.58	.00
210301_at	*XDH*	Xanthine dehydrogenase	Enzyme	3.58	.01
208323_s_at	*ANXA13*	Annexin A13	Other	3.56	.00
211253_x_at	*PYY*	Peptide YY	Other	3.55	.00
208495_at	*TLX3*	T-cell leukemia homeobox 3	Transcription regulator	3.50	.00
211900_x_at	*CD6*	CD6 molecule	Transmembrane receptor	3.50	.00
220068_at	*VPREB3*	Pre–B lymphocyte 3	Other	3.46	.00
396_f_at	*EPOR*	Erythropoietin receptor	Transmembrane receptor	3.45	.00
210483_at	*LOC254896*	Hypothetical LOC254896	Other	3.45	.00
216881_x_at	*PRB4*	Proline-rich protein *Bst*NI subfamily 4	Other	3.43	.00
220808_at	*THEG*	Theg homolog (mouse)	Other	3.42	.00
206210_s_at	*CETP*	Cholesteryl ester transfer protein, plasma	Enzyme	3.41	.00
211174_s_at	*CCKAR*	Cholecystokinin A receptor	G protein–coupled receptor	3.40	.00
220542_s_at	*PLUNC*	Palate, lung and nasal epithelium associated	Other	3.37	.00
214206_at	*PPIL6*	Peptidylprolyl isomerase (cyclophilin)-like 6	Enzyme	3.36	.00
207537_at	*PFKFB1*	6-Phosphofructo-2-kinase/fructose-2, 6-biphosphatase 1	Kinase	3.34	.00
206746_at	*BFSP1*	Beaded filament structural protein 1, filensin	Enzyme	3.34	.00
208409_at	*SLC14A2*	Solute carrier family 14 (urea transporter), member 2	Transporter	3.34	.00
215687_x_at	*PLCB1*	Phospholipase C, β 1 (phosphoinositide-specific)	Enzyme	3.34	.00
218600_at	*LIMD2*	LIM domain containing 2	Other	3.30	.00
213640_s_at	*LOX*	Lysyl oxidase	Enzyme	3.29	.00
220561_at	*IGF2AS*	Insulin-like growth factor 2 antisense	Other	3.28	.00

Table W2. (*continued*)

Affymetrix ID	Symbol	Entrez Gene Name	Type(s)	Fold Change	*P*
211483_x_at	*CAMK2B*	Calcium/calmodulin–dependent protein kinase II β	Kinase	3.21	.00
211266_s_at	*GPR4*	G protein–coupled receptor 4	G protein–coupled receptor	3.17	.00
205502_at	*CYP17A1*	Cytochrome P450, family 17, subfamily A, polypeptide 1	Enzyme	3.15	.00
222124_at	*HIF3A*	Hypoxia-inducible factor 3, α subunit	Transcription regulator	3.14	.00
208466_at	*RAB3D*	RAB3D, member RAS oncogene family	Enzyme	3.13	.00
221336_at	*ATOH1*	Atonal homolog 1 (*Drosophila*)	Transcription regulator	3.10	.00
216546_s_at	*CHI3L1*	Chitinase 3-like 1 (cartilage glycoprotein-39)	Enzyme	3.10	.00
205708_s_at	*TRPM2*	Transient receptor potential cation channel, subfamily M, member 2	Ion channel	3.09	.00
221602_s_at	*FAIM3*	Fas apoptotic inhibitory molecule 3	Other	3.09	.00
206933_s_at	*H6PD*	Hexose-6-phosphate dehydrogenase (glucose 1-dehydrogenase)	Enzyme	3.08	.00
39318_at	*TCL1A*	T-cell leukemia/lymphoma 1A	Other	3.08	.00
208130_s_at	*TBXAS1*	Thromboxane A synthase 1 (platelet)	Enzyme	3.06	.00
205487_s_at	*VGLL1*	Vestigial-like 1 (*Drosophila*)	Transcription regulator	3.06	.00
214228_x_at	*TNFRSF4*	Tumor necrosis factor receptor superfamily, member 4	Transmembrane receptor	3.04	.00
207509_s_at	*LAIR2*	Leukocyte-associated immunoglobulin-like receptor 2	Other	3.03	.00
206231_at	*KCNN1*	Potassium intermediate/small conductance calcium-activated channel, subfamily N, member 1	Ion channel	3.03	.00
216993_s_at	*COL11A2*	Collagen, type XI, α2	Other	3.01	.00
203444_s_at	*MTA2*	Metastasis associated 1 family, member 2	Transcription regulator	3.00	.00
215328_at	*EFR3B*	EFR3 homolog B (*S. cerevisiae*)	Other	2.99	.00
221350_at	*HOXC8 (includes EG:3224)*	Homeobox C8	Transcription regulator	2.98	.00
210637_at	*TACR1*	Tachykinin receptor 1	G protein–coupled receptor	2.97	.00
205468_s_at	*IRF5*	Interferon regulatory factor 5	Transcription regulator	2.95	.00
211336_x_at	*LILRB1*	Leukocyte immunoglobulin-like receptor, subfamily B (with TM and ITIM domains), member 1	Other	2.94	.00
215685_s_at	*DLX2*	Distal-less homeobox 2	Transcription regulator	2.90	.00
220485_s_at	*SIRPG*	Signal-regulatory protein γ	Other	2.88	.00
208513_at	*FOXB1*	Forkhead box B1	Transcription regulator	2.86	.00
208377_s_at	*CACNA1F*	Calcium channel, voltage-dependent, L type, α 1F subunit	Ion channel	2.84	.00
220344_at	*C11ORF16*	Chromosome 11 open reading frame 16	Other	2.83	.00
203483_at	*SEMA4G*	Sema domain, immunoglobulin domain (Ig), transmembrane domain (TM) and short cytoplasmic domain, (semaphorin) 4G	Other	2.78	.00
205733_at	*BLM*	Bloom syndrome, RecQ helicase-like	Enzyme	2.78	.00
221578_at	*RASSF4*	Ras association (RalGDS/AF-6) domain family member 4	Other	2.77	.00
220106_at	*NPC1L1*	NPC1 (Niemann-Pick disease, type C1, gene)-like 1	Transporter	2.75	.00
205820_s_at	*APOC3*	Apolipoprotein C-III	Transporter	2.75	.00
217258_x_at	*LOC100290557*	Similar to hCG91935	Other	2.74	.00
204325_s_at	*NF1*	Neurofibromin 1	Other	2.73	.00
214357_at	*C1ORF105*	Chromosome 1 open reading frame 105	Other	2.69	.00
205537_s_at	*VAV2*	Vav 2 guanine nucleotide exchange factor	Other	2.66	.00
203838_s_at	*TNK2*	Tyrosine kinase, nonreceptor, 2	Kinase	2.66	.00
207111_at	*EMR1*	Egf-like module containing, mucin-like, hormone receptor-like 1	G protein–coupled receptor	2.66	.00
214609_at	*PHOX2A*	Paired-like homeobox 2a	Transcription regulator	2.66	.00
206859_s_at	*PAEP*	Progestagen-associated endometrial protein	Other	2.66	.01
206237_s_at	*NRG1*	Neuregulin 1	Growth factor	2.65	.00
201107_s_at	*THBS1*	Thrombospondin 1	Other	2.63	.00
210184_at	*ITGAX*	Integrin, α X (complement component 3 receptor 4 subunit)	Other	2.63	.00
204948_s_at	*FST*	Follistatin	Other	2.56	.00
213724_s_at	*PDK2*	Pyruvate dehydrogenase kinase, isozyme 2	Kinase	2.56	.00
215833_s_at	*SPPL2B*	Signal peptide peptidase-like 2B	Peptidase	2.55	.00
205834_s_at	*PART1*	Prostate androgen–regulated transcript 1 (non–protein coding)	Other	2.54	.00
202895_s_at	*SIRPA*	Signal regulatory protein α	Phosphatase	2.54	.00
211312_s_at	*WISP1*	WNT1-inducible signaling pathway protein 1	Other	2.53	.00
212525_s_at	*H2AFX*	H2A histone family, member X	Other	2.51	.00
204561_x_at	*APOC2*	Apolipoprotein C-II	Transporter	2.51	.01

Table W2. (*continued*)

Affymetrix ID	Symbol	Entrez Gene Name	Type(s)	Fold Change	*P*
206273_at	*SLMO1*	Slowmo homolog 1 (*Drosophila*)	Other	2.51	.00
216963_s_at	*GAP43*	Growth-associated protein 43	Other	2.47	.00
211835_at	*IGKV1-5*	Immunoglobulin κ variable 1-5	Other	2.46	.00
209999_x_at	*SOCS1*	Suppressor of cytokine signaling 1	Other	2.45	.00
206110_at	*HIST1H3H*	Histone cluster 1, H3h	Other	2.38	.00
206917_at	*GNA13*	Guanine nucleotide binding protein (G protein), α13	Enzyme	2.38	.00
211426_x_at	*GNAQ*	Guanine nucleotide binding protein (G protein), q polypeptide	Enzyme	2.37	.00
214969_at	*MAP3K9*	Mitogen-activated protein kinase kinase kinase 9	Kinase	2.32	.01
222075_s_at	*OAZ3 (includes EG:51686)*	Ornithine decarboxylase antizyme 3	Other	2.08	.00
205017_s_at	*MBNL2*	Muscle blind-like 2 (*Drosophila*)	Other	2.02	.00

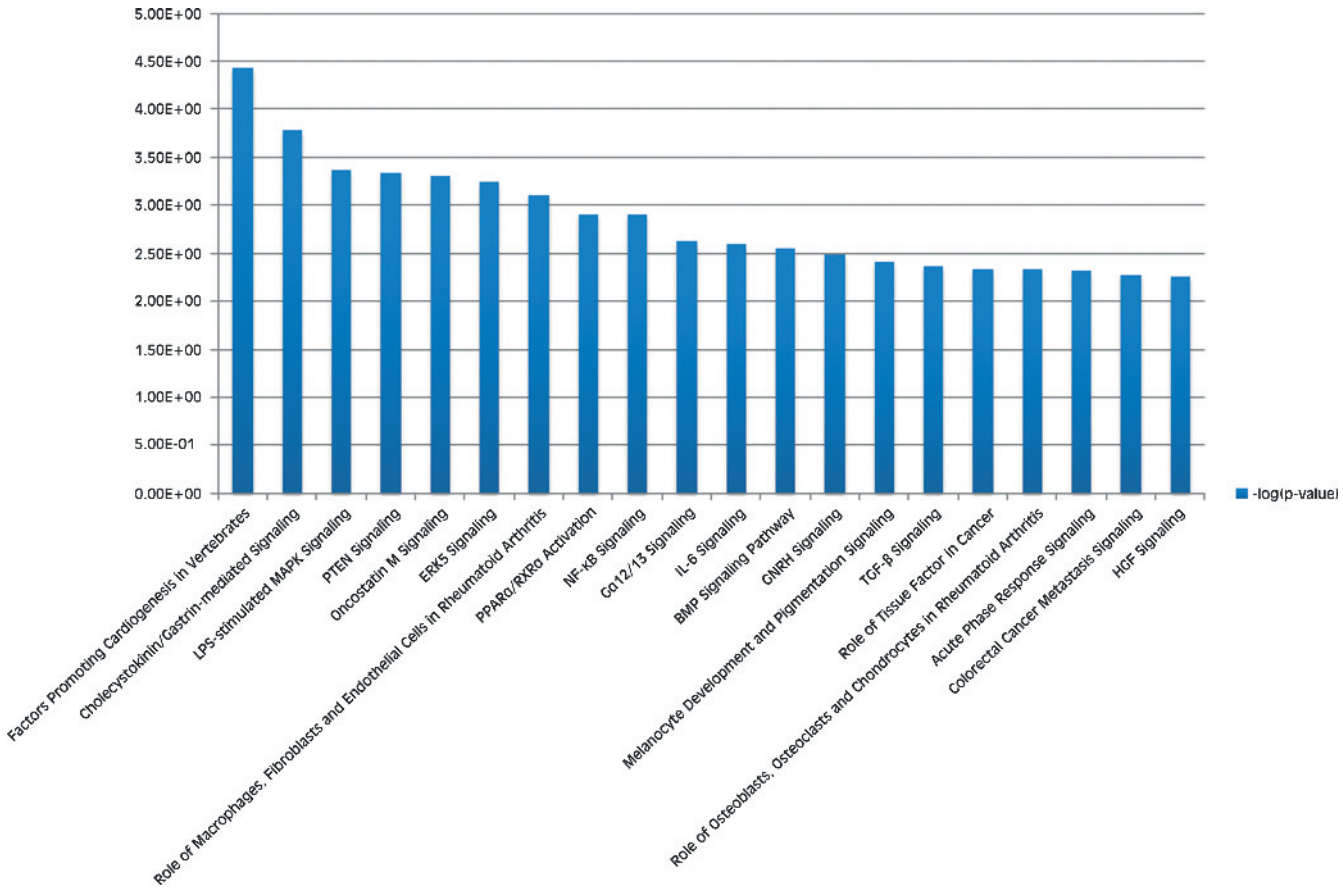

Figure W2. The top 20 significant pathways identified to be affected in VSCC. The pathways are depicted in descending order according to their significance (−log[*P*]).

Table W3. Pattern of Expression of Selected Genes in Our Series Proposed to Be Involved in Vulvar Carcinoma [15].

Affymetrix ID	Gene Symbol	Description	Fold Change	*P*	Involvement
211963_s_at	*ARPC5*	Actin-related protein 2/3 complex, subunit 5, 16 kd	1.38	<.05	P, CO
208712_at	*CCND1*	Cyclin D1	−2.6	<.05	P
216836_s_at	*ERBB2*	v-*erb*-b2 erythroblastic leukemia viral oncogene homolog 2, neuro/glioblastoma	−1.99	<.05	P, CO
211527_x_at	*VEGFA*	Vascular endothelial growth factor A	3.3	<.01	P, CO
205015_s_at	*TGFA*	Transforming growth factor, α	1.96	<.01	P
211607_x_at	*EGFR*	Epidermal growth factor receptor (erythroblastic leukemia viral (v-*erb*-b) oncogene	1.82	<.01	P
203685_at	*BCL2*	B-cell CLL/lymphoma 2	−2.58	<.01	CO
222038_s_at	*NME1*	Nonmetastatic cells 1, protein (NM23A) expressed in	1.28	<.01	CO

Genes that displayed $P < .05$ were considered significant.
CO indicates clinical outcome; P, pathogenesis and/or progression.

Table W4. The 21 Genes Upregulated Both in VIN [16] and in VSCC.

Gene Symbol	Fold Change	
	VIN	VSCC
ATAD2	8.3	2.07792
TPX2	6.2	3.61455
KIF4A	6	2.36118
MKI67	5.7	3.19299
UBE2C	5.1	2.97112
CENPE	4.7	2.40559
CDCA3	3.9	2.01355
BIRC5	3.4	2.39378
SSX2IP	3.3	2.51571
FEN1	3.2	2.14005
PRDM1	2.9	2.24525
WHSC1	2.3	2.534
H2AFX	2.3	2.07774
BLM	2.2	2.62143
NRAS	2.1	2.3029
RAD21	2	3.3336
SKP2	2	2.00554
DDX3X	1.5	3.29372
MKL1	1.3	2.4423
NCOA3	1.3	2.2841
CWF19L1	1.3	2.02551

Table W5. The 121 Genes Downregulated Both in VIN [16] and in VSCC.

Gene Symbol	Fold Change	
	VIN	VSCC
ZNF264	−1.4	−3.8994
IL11RA	−1.5	−3.05982
ZKSCAN1	−1.5	−2.9987
PARD3	−1.5	−2.81519
DALRD3	−1.5	−2.64142
NCOA1	−1.5	−2.50503
HEBP1	−1.5	−2.44703
ANXA11	−1.5	−2.08434
RPL15	−1.5	−2.03454
ALDH3A2	−1.6	−3.18065
LANCL1	−1.6	−2.24502
PGLS	−1.6	−2.04624
CPEB1	−1.6	−2.02167
NDRG2	−1.7	−3.12949
SPTBN1	−1.7	−3.03342
KIAA0495	−1.7	−2.58371
TCF4	−1.7	−2.35249
ADD1	−1.7	−2.13498
MRC2	−1.7	−2.03175
TCF7L2	−1.8	−2.92909
DIAPH2	−1.8	−2.82797
CIRBP	−1.8	−2.54922
C11orf2	−1.8	−2.3754
MSRB2	−1.8	−2.34272
TACC1	−1.8	−2.29988
SNRPN	−1.8	−2.22426
MYLIP	−1.8	−2.20568
SMARCD3	−1.8	−2.16835
CDH5	−1.8	−2.13741
NFASC	−1.8	−2.13496
GPD1L	−1.9	−5.15806
GLTSCR2	−1.9	−3.34728
GABARAPL1	−1.9	−3.24118
SESN1	−1.9	−3.11739
LRIG1	−1.9	−2.78016
VWF	−1.9	−2.5838
INPP5A	−1.9	−2.07477
MGLL	−2	−5.28424
NFIB	−2	−4.05748
KIT	−2	−3.53782
SPRY2	−2	−2.89128
PGRMC2	−2	−2.84929
CRTAP	−2	−2.20146
MPDZ	−2	−2.02107
C14orf139	−2.1	−3.10306
DDAH2	−2.1	−2.81674
TXNIP	−2.1	−2.41892
RASL12	−2.1	−2.25767
PTRF	−2.1	−2.24747
EFEMP2	−2.1	−2.04532
SFXN3	−2.1	−1.99738
EDNRB	−2.2	−4.34131
CD302	−2.2	−3.59998
ZBTB20	−2.2	−3.45299
ARMCX2	−2.2	−2.94354
PKIG	−2.2	−2.33898
SPRED2	−2.2	−2.30238
TRPC1	−2.2	−2.15492
CREB3L2	−2.2	−2.02039
HYMAI	−2.3	−4.3541
MAOB	−2.3	−3.2713
CYP3A5	−2.3	−3.15272
PGCP	−2.3	−3.04717
NR3C2	−2.3	−2.96605
ANG	−2.3	−2.43047
AXL	−2.3	−2.26289
LMO2	−2.3	−2.1959
FCGRT	−2.3	−2.1382
MAGEH1	−2.3	−2.04363
FZD7	−2.4	−7.18064
AQP1	−2.4	−4.51407
DCN	−2.4	−4.47396
GSN	−2.4	−2.25669
PLAGL1	−2.5	−9.87516
GULP1	−2.5	−8.52546
RPS6KA2	−2.5	−4.35973
MAOA	−2.5	−4.04476
ADD3	−2.5	−3.89709
CAPN3	−2.5	−3.60124
CDKN1C	−2.5	−3.27147
DAB2	−2.5	−3.19438
PHYH	−2.5	−2.61108
COL6A2	−2.5	−2.46742
CD34	−2.5	−2.19136
GHR	−2.6	−3.53847
PIK3R1	−2.6	−2.99663
MITF	−2.6	−2.98432
COX7A1	−2.6	−2.88864
FGFR1	−2.6	−2.51164
TBC1D16	−2.6	−2.18834
NR2F2	−2.7	−4.90417
PMP22	−2.7	−2.80892
NDN	−2.8	−3.53364
NRN1	−2.9	−3.29245
MAP1B	−2.9	−3.28567
PDZRN3	−3	−3.1651
SEMA6A	−3	−2.41748
FBXL7	−3	−2.39799
RNASE4	−3.1	−8.29695
FBLN1	−3.1	−7.09602
GPX3	−3.2	−9.32619
TGFBR3	−3.2	−8.56243
RBPMS	−3.2	−5.32857
CLU	−3.2	−4.61226
GPM6B	−3.2	−4.61175
OLFML1	−3.2	−3.09531
DKK3	−3.2	−2.81436
C5orf4	−3.2	−2.65594
ZNF423	−3.3	−4.38287
RAI2	−3.3	−3.6086
SGCE	−3.3	−3.33792
MLPH	−3.3	−3.30416
PPAP2B	−3.5	−4.87442
OLFML3	−3.5	−3.04505
TIMP3	−3.7	−5.33116
SLIT2	−4.1	−5.59815
AR	−4.6	−3.58597
LPHN3	−4.6	−2.1185
IGFBP6	−4.8	−4.1508
FHL1	−4.9	−8.24882
EDN3	−12.1	−15.5818

Table W5. (*continued*)